The Synthesis of Nickel Sulfide Nanoparticles on Graphitized Carbon Supports

Richard D. Tilley* and David A. Jefferson

Department of Chemistry, University of Cambridge, Lensfield Road, Cambridge CB2 1EW, U.K.

Received: February 24, 2002; In Final Form: June 3, 2002

Nickel metal nanoparticles supported on graphitized carbon have been reacted with H_2S/H_2 gas mixtures to produce catalytic nickel sulfide nanoparticles. By varying the conditions of H_2S concentration, reaction time, and reaction temperature, nanoparticles of β-Ni_3S_2, Ni_9S_8, Ni_7S_6, and β-NiS have been selectively produced. The average particle size was found to increase with conversion of the nickel metal particles to nickel sulfide particles with values that agreed with those obtained from density calculations. The phases formed were characterized by PXRD, HRTEM, and EDX and at 300 °C were those predicted from previous experiments on bulk samples. However, at 600 °C, the low-temperature phases—β-Ni_3S_2, Ni_9S_8, and Ni_7S_6—formed rather then the higher temperature phases adopted by bulk samples at this temperature.

Introduction

Because of their many potential applications in a diverse number of fields, nanoparticles have been the subject of many recent investigations.[1,2] In this study, the reaction processes of nickel nanocrystals with hydrogen sulfide were investigated.

The research in this paper falls into two sections. First, it was desired to see if by varying the conditions of reaction time, temperature and hydrogen sulfide concentration whether specific phases of nickel sulfide particles could be prepared and to elucidate a reaction scheme by which these phases form. The interest in forming nickel sulfide particles stems from their potential catalytic applications in hydrodenitrogen[3] and hydrodesulfurization processes, in particular the removal of sulfur and sulfur containing compounds from gas and oil.[3,4] Thus, the selective production of specific phases is essential for future catalytic investigations in this area.

Second, previous reports in other chalcogenide systems have shown that the structural transformations of nanocrystals differ from those of bulk phases, with particle size effects being observed. For example, Tolbert and Alivisatos in 1994[5] reported that the pressure required to produce the wurtzite-rock salt phase transition of CdSe nanocrystals was closely dependent on the particle size. Ricolleau et al. in 1999[6] also showed that the structure adopted by nanoparticles of CdS was different to that of the bulk phase, with particles smaller that 3−4 nm adopting the cubic blende-type structure as compared to particles larger than 7−8 nm which adopted the hexagonal wurtzite-type structure. For these reasons, the nickel sulfide phases formed by the nanocrystals in this study were compared to those of bulk samples.

The nickel sulfide system is highly interesting because of the number of phases that it contains, including α-$Ni_{3+x}S_2$, β-Ni_3S_2, Ni_7S_6, Ni_9S_8, α-NiS, β-NiS, Ni_3S_4, and NiS_2.[7] The system was first fully investigated by Kullerud and Yund in 1962[7] with their detailed study including a comprehensive phase diagram. Their results have recently been more accurately reassessed by Seim et al. in 1996[8] and Stolen et al. in 1994.[9] The complex structures of Ni_7S_6[10] and Ni_9S_8[11] were characterized by Fleet in 1972 and 1987, respectively, using single-crystal X-ray analysis. Note that α-$Ni_{3+x}S_2$, β-Ni_3S_2, and α-NiS are carcinogens.

Experimental Section

Preparations used nickel metal nanoparticles that had been produced on a Carbopack support formed in experiments that will be described in more detail elsewhere.[12] Summarizing, nickel nitrate, $Ni(NO_3)_2{\cdot}6H_2O$ (Fisons 99.9% purity), was dissolved in a minimum amount of distilled water and loaded onto 0.5 g of a graphitized carbon black support, Carbopack (Supelco), with a metal molar loading of 50%. The sample was then dried at 100 °C for 24 h and reduced with hydrogen gas at 300 °C for 3 h.

Sulfuridization was achieved by reacting samples of nickel metal nanoparticles in a furnace with 10% and 1% H_2S/H_2 gas mixtures at 300 and 600 °C with a flow rate of approximately 50 std cm^3 min^{-1} (gases used, 10% hydrogen sulfide (Messer) diluted with H_2 (Messer) for 1% reactions). Reaction temperatures of 300 and 600 °C were chosen because the nickel sulfide system has several phases only stable below 400 °C. These include stoichiometric β-NiS which is stable below 379 °C and Ni_9S_8 which is stable below 400 °C.[7] Thus, experiments at 300 °C were designed to form nanoparticles of these lower temperature phases and those at 600 °C to form the higher temperature phases. For preparations at 300 °C, the sample was allowed to cool under the flow of gas until the temperature had dropped to below 70 °C before removal from the furnace, to prevent any oxidation, and this normally took approximately 20 min. For experiments at 600 °C, the preparations were quenched, this being achieved by maintaining the temperature and changing the gas so that nitrogen flowed through the furnace instead of the H_2S/H_2 mixture. Nitrogen was allowed to flow for 20 min to purge the furnace of hot hydrogen, which was then opened, and the sample crucible removed onto a metal block thus quickly cooling the preparation.

Preliminary characterization of all samples employed X-ray powder diffraction, using a STOE diffractometer with a horizontal goniometer and Cu Kα radiation ($\lambda = 0.1542$ nm.). Peaks due to sulfide particles were indexed, and particle size analysis using the Scherrer equation was carried out. Specimens

* To whom correspondence should be addressed. RDT present address, Advanced Materials Laboratory, Toshiba RDC center, 1, Komukai Toshiba-Cho, Saiwai-ku, Kawasaki 212-8582, Japan. E-mail: richard.tilley@glb.toshiba.co.jp.

10.1021/jp0256847 CCC: $22.00
Published on Web 10/01/2002

TABLE 1: Reaction Conditions and Products of Experiments in which Nickel and Nickel Sulfide Nanoparticles on a Graphitized Carbon Support Were Reacted with Hydrogen Sulfide

expt	starting material	P_{H2S}/P_{H2}	time (h)	temp (°C)	products
A	nickel metal	10%	1.5	600	Ni_7S_6(major) Ni_9S_8(minor)
B	nickel metal	10%	7	600	Ni_9S_8(major) Ni_7S_6(minor)
C	nickel metal	10%	13	600	Ni_9S_8
D	nickel metal	10%	3	300	Ni_9S_8 and β-NiS
E	nickel metal	10%	10	300	β-NiS
F	nickel metal	1%	6	600	β-Ni_3S_2 and nickel metal
G	nickel metal	1%	6	300	β-Ni_3S_2 and nickel metal
H	nickel metal	100 ppm	13	600	No reaction
I	nickel metal	100 ppm	13	300	No reaction
J	β-Ni_3S_2 and nickel metal	10%	6	600	Ni_9S_8(major) Ni_7S_6(minor)
K	Ni_9S_8	10%	6	300	β-NiS
L	Ni_7S_6(major) Ni_9S_8(minor)	10%	6	600	Ni_9S_8

for electron microscopy were prepared directly from the product material by suspension in acetone and transferring to a gold grid coated with an amorphous carbon support. HRTEM images were recorded on a JEOL JEM-3011 electron microscope with a LaB_6 cathode operated at 300 keV. Images were recorded photographically at magnifications ranging from 3 to 600 000X and were then digitized for subsequent analysis. Digital image processing and fast Fourier transform formation was performed using SEMPER 6+ software. Computer-simulated electron diffraction patterns were obtained from CARINE 3.1 software. The JEM-3011 was fitted with a PGT-XS14 energy-dispersive X-ray (EDX) detector and AVALON associated analytical system. Calibration of detector sensitivity for S Kα and Ni Kα radiation was effected by the use of several bulk sulfides including α-NiS and NiS_2, which were confirmed as single phase by X-ray powder diffratometry.

Identification of individual nanoparticles in the electron microscope using nanobeam diffraction techniques proved impractical, partly because of rapid contamination of the specimen when the microscope was being used in nanobeam mode but also because of the very high background level of diffraction from the supporting medium which made the pattern of the particles difficult to resolve. Particle characterization was therefore achieved by obtaining a power spectrum from a fast Fourier transform of the high-resolution lattice fringe images, which had the advantage that the resulting pattern contained little contribution from the support. This power spectrum was then compared to a simulated diffraction pattern from a model of the specimen under analysis.

To identify the nanocrystals observed in electron micrographs, it was necessary to measure the lattice fringes on the particles to a high degree of precision. Use of the power spectrum was preferred to actual measurement of fringe spacings in the image because it was intrinsically more accurate and avoided the parallex errors invariably present in measurement of fringe spacings manually. Calibration of the spacing between lattice fringes on the nanocrystals was obtained by a comparison with the known spacings of the graphitized carbon support which display fringes with lattice spacings 0.344 nm from the (002) planes and 0.213 nm from the (100) planes.

Results and Discussion

The results from powder X-ray diffraction (PXRD) analysis are summarized in Table 1. The patterns from the products of experiments A, B, and C which had reaction conditions of 10% hydrogen sulfide and 600 °C indicated that with shorter reaction times, 1.5 h, Ni_7S_6 forms as the major product with Ni_9S_8 as a minor phase. At longer reaction times, the amount of Ni_9S_8 increases until after 13 h Ni_9S_8 nanoparticles form as the single phase product (experiment C). Thus, Ni_9S_8 appears to be the thermodynamically stable product under these conditions. The fact that the low-temperature phase, Ni_9S_8, formed at 600 °C was surprising as Ni_9S_8 has been found to be stable only up to about 400 °C in bulk investigations.[7] PXRD data from experiments D and E, which had reaction temperatures of 300 °C, indicate that Ni_9S_8 was the major phase and β-NiS the minor phase present at a short reaction time of 3 h and with β-NiS single phase product after a longer reaction time of 10 h. These results are in agreement with bulk investigations which found that both of these phases are stable at 300 °C.[7] Several additional experiments using lower hydrogen sulfide concentration and reaction times under 3 h were tried, but Ni_7S_6 was not found to form at this temperature. Powder patterns of experiments F and G with 1% hydrogen sulfide showed that both samples had only partially reacted with hydrogen sulfide to form β-Ni_3S_2 nanoparticles with some unreacted nickel metal particles remaining. Again the formation of β-Ni_3S_2 at 600 °C differs from results of bulk studies with α-Ni_3S_2 being the stable higher temperature phase. The PXRD pattern of experiments A, E, and F are shown in Figures 1−3, respectively.

Three further experiments were carried out to confirm that the nickel sulfide nanoparticles formed in the above experiments could be converted to more sulfur-rich sulfides by further reaction with hydrogen sulfide. PXRD data from experiment J proved that β-Ni_3S_2 nanoparticles could be further reacted to form Ni_9S_8 and Ni_7S_6 particles, experiment K proved that Ni_9S_8 nanoparticles could be converted to β-NiS nanoparticles, and experiment L proved that Ni_7S_6 nanoparticles could be further sulfided to produce Ni_9S_8 nanoparticles.

Energy-Dispersive X-ray Spectroscopy. EDX spectroscopy was used to obtain the overall composition of the products of each of the above experiments by recording approximately 40 spectra from different crystals. The compositions found agreed with the X-ray diffraction data. The EDX spectra of the individual particles shown in Figures 4−6 are shown in each figure.

High-Resolution Transmission Electron Microscope. HRTEM images of many of the particles could be characterized, with image interpretation being achieved by matching the computer simulated power spectrum with the power spectrum of the image. These include the particles of Ni_9S_8, β-NiS, and β-Ni_3S_2 shown in Figures 4−6, respectively. Previous studies investigating the reaction of platinum with low concentrations of hydrogen sulfide found that platinum nanoparticles reconstructed in the presence of sulfur to form cubic particles with a thin sulfide surface layer.[13,14] Electron microscope studies of experiments F and G which had products of β-Ni_3S_2 and unreacted nickel metal found no partially reacted particles or particles with an obvious sulfide coating. All crystalline particles observed were either entirely β-Ni_3S_2 or unreacted nickel metal.

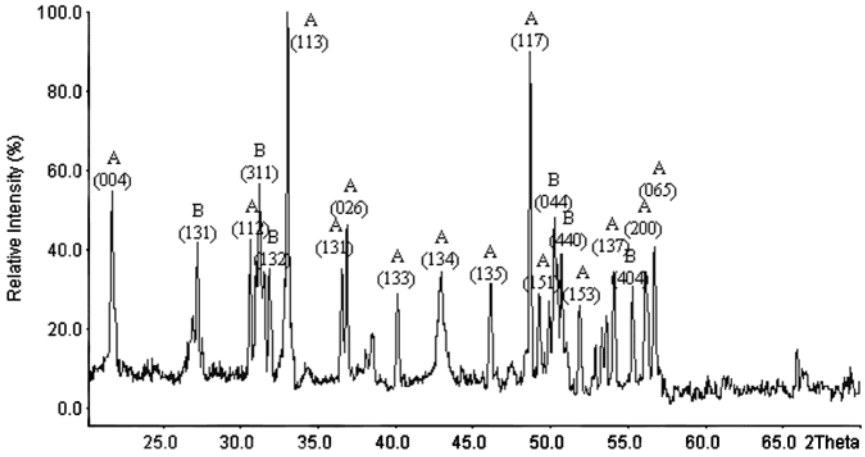

Figure 1. Powder X-ray diffraction pattern of nickel metal particles reacted with 10% hydrogen sulfide at 600 °C for 1.5 h, experiment A. A = Ni_7S_6 and B = Ni_9S_8.

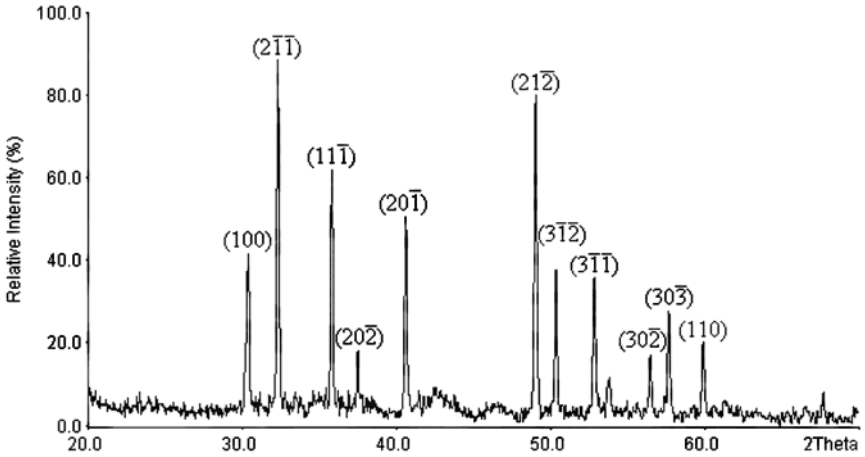

Figure 2. Powder X-ray diffraction pattern for nickel nanoparticles reacted with 10% hydrogen sulfide at 300 °C for 10 h, experiment E. The peaks were assigned to β-NiS.

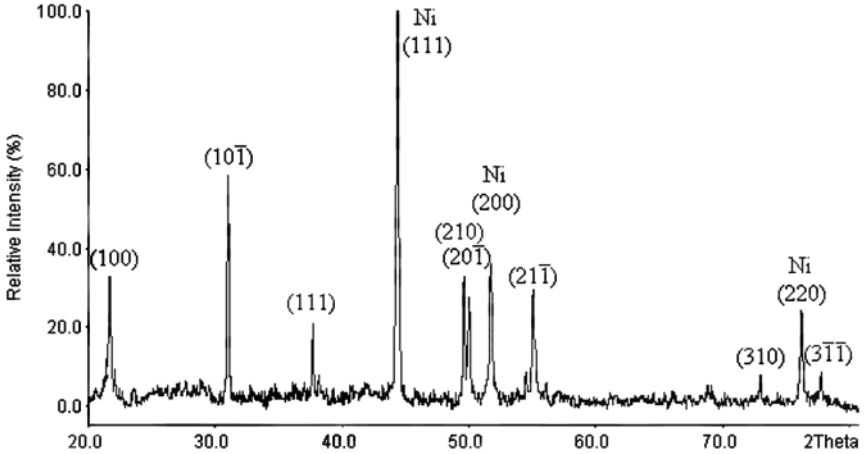

Figure 3. Powder X-ray diffraction pattern of nickel nanoparticles reacted with 1% hydrogen sulfide at 600 °C for 6 h, experiment F. The peaks were assigned to β-Ni_3S_2 and nickel metal.

It was thus concluded that once the initial sulfiding reaction has started it must happen very quickly and goes rapidly to completion. It was also noted that in all experiments (A−K) about 10% of the particles examined were semicrystalline or amorphous. It is possible that these are particles are in the process of converting from one phase to another.

Reaction Sequence. There are two possible routes of formation for the nickel sulfide nanoparticles. Either they can form directly with hydrogen sulfide to produce β-Ni_3S_2, Ni_9S_8, Ni_7S_6, and β-NiS or there can be a sequence of reactions in which a lower sulfide such as β-Ni_3S_2 initially forms which then goes on to react sequentially with hydrogen sulfide to produce more sulfur-rich sulfides. From the results, particularly those of experiments J, K, and L, it may be concluded that it is this sequential process that occurs as outlined in Scheme 1. These results agree with previous studies on bulk samples whichhave shown that bulk nickel sulfide samples can interconvert when reacted with H_2/H_2S gas mixtures.[15,16]

Nickel Sulfide Particle Size. For each experiment, the average particle size was calculated by applying the Scherrer

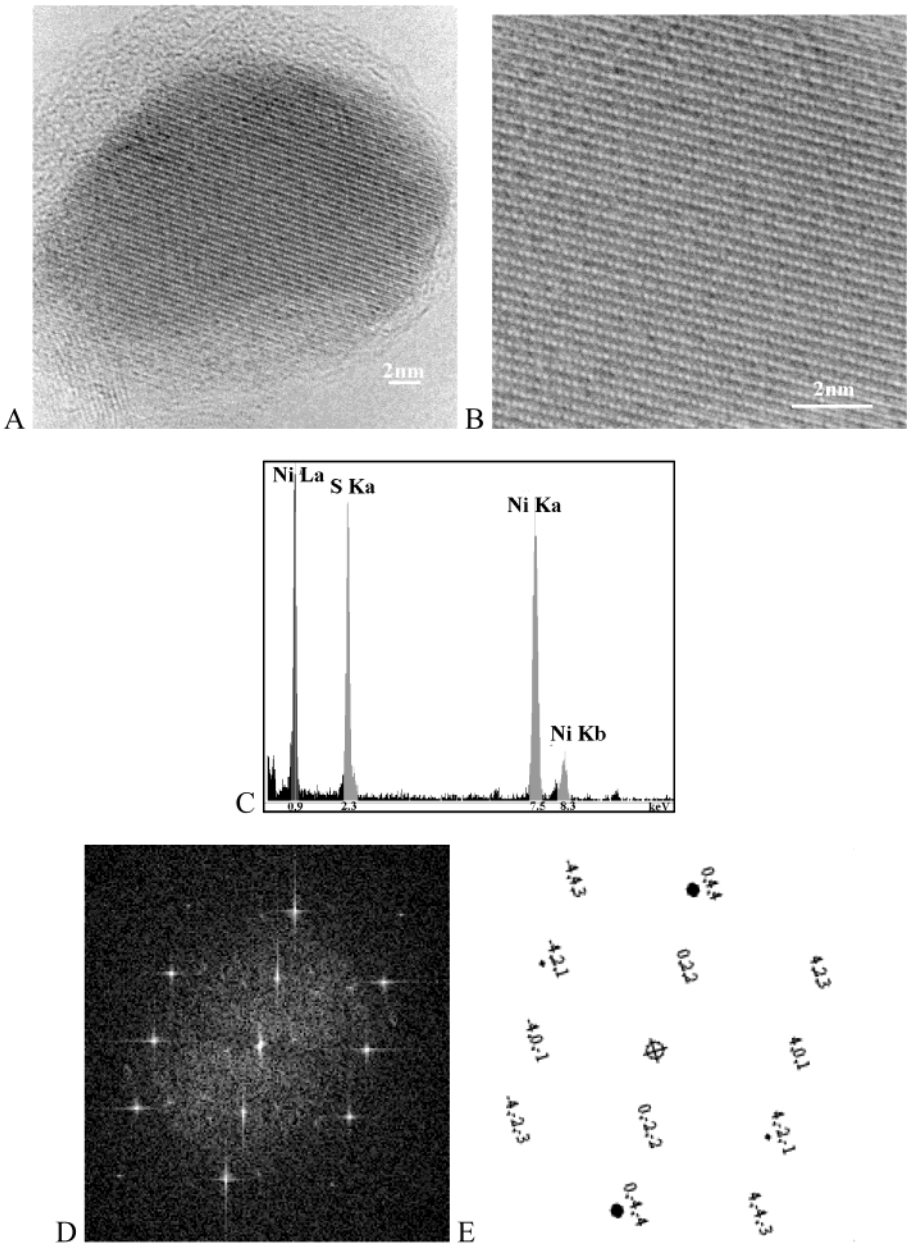

Figure 4. Image of a 21 nm particle of Ni_9S_8, A and B, which is roughly spherical and has an amorphous coating. The graphitized carbon support is also visible in the bottom left of the micrograph. Energy dispersive spectroscopy spectrum (C) measured a composition of $Ni_{8.9+0.8}S_8$. Power spectrum (D) and matching computer simulation of N_9S_8 (E) projected down the [144].

SCHEME 1: Reaction Sequence for Nickel Metal Nanoparticles Reacted with Hydrogen Sulfide at 600 and 300 °C. The Scheme Shows that at Both Temperatures Nickel Particles First Transform into β-Ni_3S_2 Particles, Which Then Sequentially React with Greater Concentrations of Hydrogen Sulfide to Produce More Sulfur Rich Sulfides

600 °C Nickel → β-Ni_3S_2 → Ni_7S_6 → Ni_9S_8

300 °C Nickel → β-Ni_3S_2 → Ni_9S_8 → β-NiS

equation to the peak broadening of the powder diffraction peaks. Generally, the calculations indicated an average particle size of between 40 and 60 nm. Electron microscope observations confirmed these figures with the size of a typical particle being approximately 50 nm and a size distribution of 2−100 nm found for all experiments. The nickel nanoparticle reagents generally had an average particle size of 20 nm and variation in size of 1−50 nm as observed in the electron microscope. It was predicted that, upon reaction of the nickel metal particles with hydrogen sulfide, there would be an increase in the average particle size, because the density of nickel metal atoms in nickel sulfides is less than in nickel metal. Table 2 shows the calculated values and experimental values of the nickel sulfide particle sizes for several experiments. From the results in the table, it can be seen that there is an excellent correlation between the expected growth and that found in experiments. This is also an indication that there was little additional particle growth because of heating.

Comparison with Studies on Bulk Samples. The nickel sulfide products of this nanoparticle study can best be interpreted by two comparisons with the equilibrium products expected from bulk samples. First, to establish which phases are stable at 300 and 600 °C, a comparison can be made with the phase diagram of the nickel sulfide system as reported by Kullerund and Yund in 1962[7] and confirmed by more recent studies of Seim et al. in 1996[8] and Stolen et al. in 1994.[9] Second, an assessment of which products should be formed with 1% and

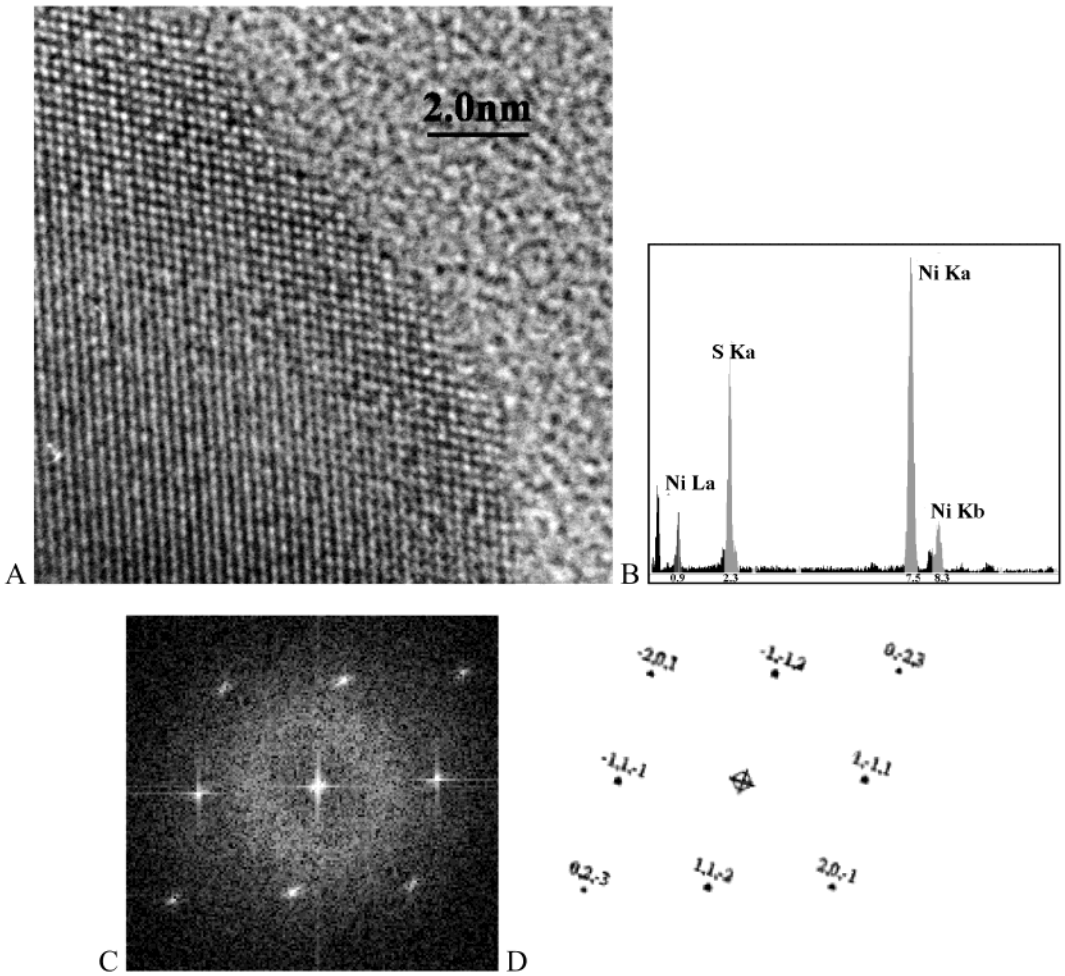

Figure 5. Part of an image of a 29 nm β-NiS nanoparticle (A). Energy dispersive spectroscopy spectrum (B) measured a composition of $Ni_{0.95+0.08}S$. Power spectrum (C) and matching simulation of β-NiS projected down the [132] direction.

10% P_{H2S}/P_{H2} at 300 and 600 °C can be achieved from calculations using the Gibbs free energies recorded for bulk samples by Rosenqvist in 1954. Equilibrium conditions or close to equilibrium conditions can be assumed to be attained because of the small particle sizes and hence the short diffusion distances involved.

For the first comparison, the temperature ranges which the nickel sulfide phases Ni_9S_8, Ni_7S_6, and β-Ni_3S_2 form, according to the thermodynamic literature,[7−9,16,17] are summarized in Table 3. As reported in the table, the Ni_9S_8 to Ni_7S_6 phase transition has been reported to occur at 400[7] and 406 °C.[9] Ni_7S_6 has been reported to decompose to α-$Ni_{3+x}S_2$ and $\alpha-$NiS at 560,[16] 573,[7] and 577 °C.[9] The phase transition of β-Ni_3S_2 to α-$Ni_{3+x}S_2$ has been found to occur at 555,[16] 556,[7] and 565 °C.[17] Thus according to the literature, the experiments at 600 °C should have produced either α-$Ni_{3+x}S_2$ or α-NiS or a mixture of the two rather than the lower temperature phases of β-Ni_3S_2, Ni_9S_8, and Ni_7S_6 that were actually observed. At 300 °C, the products of β-Ni_3S_2, Ni_9S_8, and β-NiS agree with those expected from the phase diagram.

For the second comparison, the equilibria for the reaction of nickel with hydrogen sulfide are

$$3/2Ni + H_2S = 1/2Ni_3S_2 + H_2$$

$$2Ni_3S_2 + H_2S = Ni_6S_5 + H_2$$

$$Ni_6S_5 + H_2S = 6NiS + H_2$$

Ni_6S_5 has been included in the scheme above instead of the two phases Ni_7S_6 and Ni_9S_8 because Rosenqvist referred to these two phases collectively as Ni_6S_5. Using the thermodynamic data[16] in Table 4, the equilibrium value of P_{H2S}/P_{H2} may be calculated.

Table 5 reports the expected products from these comparisons with the thermodynamic literature.[7−9,16] From the results at 300 °C, it can be concluded that the experimental products for nanoparticles found in these investigations are the same as those found for bulk samples. However, at 600 °C, lower temperature phases are formed by nanoparticles rather than the higher temperatures phases formed by the bulk samples.

Stabilization of Nickel Sulfide Phases to Higher Temperatures. The results in this study indicate that the phases β-Ni_3S_2, Ni_7S_6, and Ni_9S_8 are stabilized with respect to the phase α-$Ni_{3+x}S_2$ because it is these former phases that are produced at higher temperatures rather than the α-$Ni_{3+x}S_2$ which is formed in bulk experiments. There are several possibilities for the cause of this stabilization, such as an interaction from the support or simply the nanoparticulate nature of the samples. As mentioned in the Introduction, previous studies on chalcogenide nanocrystals have shown that phase transitions can be affected by particle size, with the pressure-induced wurtzite-rock salt phase transition of CdSe nanocrystals[5] and the structures adopted by CdS nanocrystals[6] being closely dependent on this parameter. If the stabilization of nickel sulfide phases in this study to higher temperatures is also a size dependent factor, then the thermodynamics of the phase transitions must be

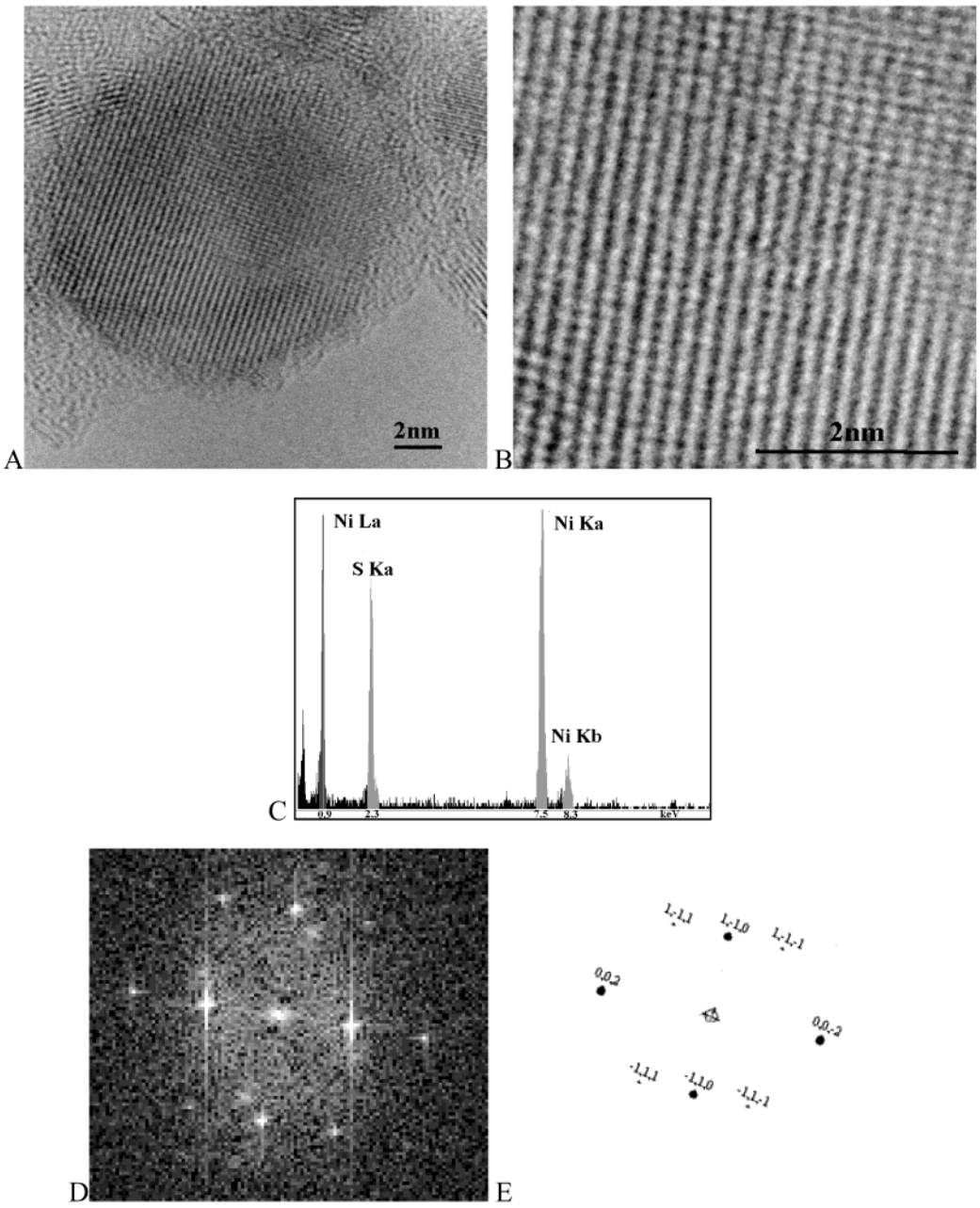

Figure 6. Electron microscope image, A and B, of a 16 nm β-Ni_3S_2 nanoparticle. Energy dispersive spectroscopy spectrum (C) measured a composition of $Ni_{3.1+0.1}S_2$. Power spectrum (D) and matching computer simulation (E) of β-Ni_3S_2 projected down [110].

TABLE 2: Calculated Values and Experimental Values of Increase in Size of Nickel Sulfide Particles[a]

phase	nickel atom density (atom/Å)	nickel metal particle size (nm; starting material)	calcd nickel sulfide particle size (nm)	expt nickel sulfide particle size (nm)	
Ni metal	0.0900				
β-Ni_3S_2	0.0440	22	45	46	(expt G)
Ni_7S_6	0.0375	23	55	59	(expt A)
Ni_9S_8	0.0365	23	57	60	(expt A)
Ni_9S_8	0.0365	20	49	49	(expt C)
β-NiS	0.0358	20	50	56	(expt E)

[a] The calculated values were obtained from the average size of the nickel metal nanoparticles in the starting material and the density of nickel metal atoms in the nickel sulfide.[7,10,11]

considered. In the nickel sulfide system, the thermodynamic driving force for the transition of the phases β-Ni_3S_2, Ni_7S_6, and Ni_9S_8 into α-$Ni_{3+x}S_2$ is predominantly the gain in entropy.

TABLE 3: Temperature Ranges in Which the Nickel Sulfides Ni_9S_8, Ni_7S_6, and β-Ni_3S_2 Form According to the Authors Listed

phase	author	temperature range
Ni_9S_8	Kullerud and Yund (1962)	below 400 °C
Ni_9S_8	Stolen et al. (1994)	below 406 °C
Ni_7S_6	Kullerud and Yund (1962)	above 401 °C below 573 °C
Ni_7S_6	Stolen et al. (1994)	above 406 °C below 577 °C
β-Ni_3S_2	Fjellvag and Andersen (1994)	below 565 °C
β-Ni_3S_2	Kullerud and Yund (1962)	below 556 °C
β-Ni_3S_2	Rosenqvist (1954)	below 555 °C

The α-$Ni_{3+x}S_2$ structure has sulfur atoms in a face-centered cubic array with the nickel atoms statistically distributed over the metal sites.[7] This random distribution of metal atoms and therefore vacancies leads to an increase in entropy in comparison to the structures of β-Ni_3S_2, Ni_7S_6, and Ni_9S_8. However, for nanoparticles, the role of the surface must also be considered. As with the thermodynamics of the bulk solids, disorder of vacancies

TABLE 4: Literature Values for ΔG° (J) from Rosenqvist[16] and the Calculated Values of P_{H2S}/P_{H2} at 600 and 300 °C[a]

equilibrium	ΔG° (Joules)	equilibrium P_{H2S}/P_{H2} at 600 °C calculated	equilibrium P_{H2S}/P_{H2} at 300 °C calculated
$3/2Ni + H_2S = 1/2Ni_3S_2 + H_2$	$-75{,}530 + 32.2T$	0.14%	0.00061%
$2Ni_3S_2 + H_2S = Ni_6S_5 + H_2$	$-12{,}770 - 7.75T$	6.7%	2.7%
$Ni_6S_5 + H_2S = 6NiS + H_2$	$-21{,}860 + 14.5T$	28%	5.8%

[a] Note, in experiments, P_{H2S}/P_{H2} values of 1% and 10% were used.

TABLE 5: Expected Sulfide Products from the Thermodynamic Literature and the Experimental Products Obtained from Reactions at 300 and 600 °C

	1% P_{H2S}/P_{H2}	10% P_{H2S}/P_{H2}	P_{H2S}/P_{H2} value for the formation of β-NiS
expected results for bulk samples at 300 °C[7-9,16]	β-Ni_3S_2	Ni_9S_8	12%
experimental results at 300 °C	β- Ni_3S_2	Ni_9S_8 and β-NiS	β-NiS formed at 10% H_2S/H_2
expected results for bulk samples at 600 °C[7-9,16]	α- $Ni_{3+x}S_2$	α-$Ni_{3+x}S_2$	25%
experimental results at 600 °C	β-Ni_3S_2	Ni_9S_8	α-NiS did not form at 10% H_2S/H_2

on the surface will provide a positive entropy contribution. The fact that low-temperature phases were stabilized to higher temperatures may suggests that for nanoparticles this surface entropy consideration is more significant than the role of bulk vacancies.

Conclusions

The results in this study show that nickel nanoparticles on a Carbopack support may be reacted with hydrogen sulfide to produce nanocrystals of the nickel sulfides β-Ni_3S_2, Ni_7S_6, Ni_9S_8, and β-NiS. These nickel sulfide phases may be selectively formed by varying the reaction conditions of hydrogen sulfide concentration, temperature, and time. A reaction sequence has been identified with the nickel sulfide phase β-Ni_3S_2 initially forming with low P_{H2S}/P_{H2} concentrations and progressively reacting with hydrogen sulfide to produce more sulfur rich nickel sulfides.

The nanoparticles in this study were also found to form with phases different to those of the bulk sulfides with the low-temperature phases β-Ni_3S_2, Ni_9S_8, and Ni_7S_6 being stabilized to higher temperatures. This could be due to the nanoparticular nature of the samples; however, further experiments and theoretical calculations would have to be performed to fully elucidate the true cause of this discovery.

Acknowledgment. We thank the EPSRC for funding this research. Financial support for R.D.T. was also obtained from JEOL (UK) Ltd and the Isaac Newton Trust, and this is gratefully acknowledged.

References and Notes

(1) New Aspects of Nanocrystalline Research. *MRS Bull.* **2001**, *26*, 981−1019.
(2) Nanotech: Special Issue. *Sci. Am.* Sept **2001**, *285*, 26−78.
(3) Cid, R.; Atanasova, P.; Lopez-Cordero, R.; Palacios, J. M.; Lopez-Agudo, A. *J. Catal.* **1999**, *182*, 328.
(4) Welters, W. J. J.; Vorbeck, G.; Zandbergen, H. W.; de Haan, J. W.; van Santen, R. A. *J. Catal.* **1994**, *150*, 155.
(5) Tolbert, S. H.; Alivisatos, A. P. *Science* **1994**, *265*, 373.
(6) Ricolleau, C.; Audinet, L.; Gandais, M.; Gacoin, T. *Euro. Phys. J. D* **1999**, *9*, 565.
(7) Kullerud, G.; Yund, R. A. *J. Petrol.* **1962**, *3*, 126.
(8) Seim, H.; Fjellvag, H.; Gronvold, F.; Stolen, S. *J. Solid State Chem.* **1996**, *121*, 400.
(9) Stolen, S.; Fjellvag, F.; Gronvold, F.; Seim, H.; Westrum, E. *J. Thermodynamics* **1994**, *26*, 987.
(10) Fleet, M. E. *Acta Crystallogr.* **1972**, *B28*, 1237.
(11) Fleet, M. E. *Acta Crystallogr.* **1987**, *C43*, 2255.
(12) Tilley, R. D.; Jefferson, D. A. *J. Mater. Chem.*, in press.
(13) Harris, P. J. F. *Nature* **1986**, *323*, 792.
(14) Jefferson, D. A.; Harris, P. J. F. *Nature* **1988**, *332*, 617.
(15) Kiuchi, H.; Funaki, K.; Tanaka, T. *Metall. Mater. Trans. B* **1983**, *14*, 347.
(16) Rosenqvist, T. *J. Iron Steel Res. Inst.* **1954**, *176*, 37.
(17) Fjellvag, H.; Andersen, A. *Acta Chem. Scand.* **1994**, *48*, 290.